Spring 5-2-2023

Is VDAC1 a Novel BCL2 Family Member that Binds BAX?

Claire Pearson

IS VDAC1 A NOVEL BCL2 FAMILY MEMBER THAT BINDS BAX?

by

Claire Pearson

A thesis submitted to the faculty of The University of Mississippi in partial fulfillment of the requirements of the Sally McDonnell Barksdale Honors College.

Oxford
April 2023

Approved by

_____
Advisor: Dr. Mika Jekabsons

_____
Reader: Dr. Bradley Jones

_____
Reader: Dr. Robert Doerksen

ACKNOWLEDGEMENTS

ABSTRACT

Apoptosis is a type of regulated cell death important for normal embryonic development and maintenance of adult tissues by removing excess or dysfunctional cells to ensure proper functioning of organs. The Bcl-2 family of proteins determines whether apoptosis remains suppressed or becomes activated through the balance of interactions among pro-survival and pro-death members. A defining feature of the Bcl-2 family is a BH3 domain that drives interactions between the family members. Isoform 1 of the voltage dependent anion channel (VDAC1) has an important role in metabolism, but was recently found to have high homology with known BH3 domains. This study tested the hypothesis that VDAC1 has a BH3 domain at its N-terminus, making it a novel member of the Bcl-2 family. The ability of the pro-death family member Bax to bind a panel of wild type and mutant VDAC1 peptides was tested to determine if VDAC1 contains a functional BH3 domain, and the residues most important for driving this interaction. The mutant peptides were developed to substitute two or more of the seven hydrophobic residues (designated H_0-H_5) with those having less hydrophobicity, or replacing a conserved aspartate with arginine. Equilibrium binding of fluorescent-tagged peptides to recombinant Bax was assessed by separating free from bound peptide with spin filters. The two most important residues that promoted VDAC1 interaction with Bax were the conserved aspartic acid, and a hydrophobic proline at 'H_0'. The lower affinity of Bax for VDAC1 compared to the known Bim BH3 domain is likely due to the non-conserved position of the hydrophobic H_2 leucine creating steric interference with the close proximity H1 tyrosine. The binding analysis supports the hypothesis that VDAC1

iv

possesses a BH3 domain, although the sequence of the domain is less well suited to

interaction with Bax compared to the Bim BH3 domain.

TABLE OF CONTENTS

LIST OF TABLES AND FIGURES

INTRODUCTION

Apoptosis is the pathway by which a cell undergoes programmed cell death to rid the body of dysfunctional and damaged cells, or excess cells resulting from over-proliferation of progenitor cells during development. If a cell is prevented from undergoing apoptosis, it can lead to accumulation of genetic mutations, uncontrolled cell division, and the development of a tumor (NIH). The regulators of the apoptotic pathway are a group of related proteins commonly known as the B cell lymphoma-2 (Bcl-2) family (Siddiqui et al, 2015). The members of the Bcl-2 family are related by their Bcl-2 homology (BH) domains that are characterized by regions of conserved sequences. The BH domains facilitate the family members' interactions with each other to either stimulate or inhibit apoptosis (Warren et al, 2019). The Bcl-2 family is divided into three groups based on their role in apoptosis: (1) anti-apoptotic proteins (e.g., Bcl-2, Bcl-xL, Mcl-1), (2) pro-apoptotic pore-formers (Bax and Bak), and (3) pro-apoptotic BH3-only proteins (e.g., Bim, Bid, Bad) (Kale et al, 2018). All Bcl-2 family members contain a BH3 domain; one of the four BH domains (BH1, BH2, BH3, BH4) involved in interactions between these proteins (Lomonosova & Chinnadurai, 2008). For the 'multi-domain' family members, the BH1, BH2, and BH3 motifs are arranged into a hydrophobic groove into which the BH3 domain of another member can bind, while the BH4 motif lies at the N-terminus (Birkinshaw and Czabotar, 2017).

The basic pathway of apoptosis in vertebrates begins with permeabilization of the mitochondrial outer membrane (MOM) by proapoptotic members of the Bcl-2 family (Douglas R. Green, 2005). The Bcl-2 family member Bax is activated by one or more BH3-only proteins binding to the inactivate monomer, which triggers a series of

conformational changes that trigger Bax oligomerization and formation of pores in the
mitochondria, causing mitochondrial outer membrane permeabilization (MOMP) (Adams
& Cory, 1998) (Kale et al, 2018). In healthy, non-apoptotic cells, Bax is localized in the
cytosol predominantly, but can also be found in small amounts in the MOM and the
endoplasmic reticulum in an inactive conformation (Hsu & Youle, 1998) (Hsu et al,
1997). Upon exposure to a stressor, Bax translocates from the cytosol, to the
mitochondria where it adopts an active conformation which results in MOMP (Renault &
Manon, 2011) (Wolter et al, 1997). Activation of Bax is the result of a multistep process
in which its α2 helical BH3 domain becomes exposed, and the helix α9 leaves the
hydrophobic groove to insert into the mitochondrial outer membrane (Guedes et al,
2022). In the activated, membrane anchored state, the exposed hydrophobic groove of
Bax, can bind other BH3 domains, which either, stimulates oligomers to form (some
BH3-only proteins) or prevent activation by forming stable heterodimers with Bax (Bcl-
xL, Bcl-2) (Guedes et al, 2022). The former process leads to MOMP which in turn results
in cell death (Lalier et al, 2007).

     The voltage-dependent anion channel 1 (VDAC1) is an important regulator of
mitochondrial function, and serves as a mitochondrial gatekeeper, by allowing small
metabolites such as pyruvate and ATP to pass between the cytoplasm and mitochondrial
intermembrane space (Shoshan-Barmatz et al, 2020). VDAC1 is composed of 19
transmembrane β-strands connected by flexible loops form a B-barrel with a 25-residue-
long N-terminal region located inside the pore (Bayrhuber et al, 2008) (Hiller et al, 2008)
(Ujwal et al, 2008). It has been proposed that the N-terminus can move from the internal
pore to the cytoplasm (Hiller et al, 2009) (Geula et al, 2012). This leaves the N-terminus

ideally positioned to regulate the conductance of ions and metabolites which pass through the VDAC1 pore (Ujwal et al, 2008). The mobility of the N-terminal region has been suggested to be involved with channel gating, interaction with anti-apoptotic proteins, and VDAC1 dimer formation (Guela et al, 2012). This also is proposed to serve as the interaction site of apoptosis-regulating proteins of the Bcl-2 family (Bax, Bcl-2, and Bcl-xL) and hexokinase (HK) (Abu-Hamad et al, 2009) (Shi et al, 2003) (Arbel et al, 2012) (Arzoine et al, 2009).

While the exact role of VDAC1 in apoptosis is still not understood, some studies have found that it alleviates apoptosis in part by binding with hexokinase II (HKII), which prevent pro-apoptotic proteins (eg. Bax) from binding to the MOM (Camara et al, 2010, 2011). Another function of VDAC1 in apoptosis has been proposed to be that the protein regulates apoptosis via mediating the release of apoptotic proteins from the mitochondria. Apoptotic and pathological conditions induce cell death by inducing VDAC1 overexpression leading to oligomerization, and the formation of a large channel within the VDAC1 homo-oligomer. This permits the release of pro-apoptotic proteins from the mitochondria and subsequent apoptosis (Shoshan-Barmatz et al, 2020). However, unpublished data from the Jekabsons lab discovered that the VDAC1 N-terminal sequence is highly homologous to known BH3 domains (Pandey et al, manuscript in preparation). This could explain how VDAC1 may interact with Bax or other Bcl-2 family members, and raises the possibility that VDAC1 is a novel member of the Bcl-2 family.

This study seeks to understand if VDAC1 contains a functional BH3 domain. The role of specific amino acids within the putative VDAC1 BH3 domain was systematically analyzed using a series of mutant peptides and their ability to bind to recombinant Bax.

METHODS

A. Recombinant Bax

Recombinant human Bax was purchased from Creative Biomart (Shirley, New York, catalog number = Bax-6976H). It contains His-tags on both the N- and C- terminus and is truncated at Gln171 (final 21 residues deleted) to remove the 9th alpha helix. This improves protein solubility and exposes the hydrophobic groove for peptide binding analysis.

B. Synthetic peptides

Wild type and mutant Bim and VDAC1 custom 26-mer peptides (90% purity) were purchased from Mimotopes, Inc. (Victoria, Australia). All peptides were tagged at the N-terminus with carboxyfluorescein containing an aminohexanoic acid linker. Bim peptide was dissolved in 80 mM NH_4HCO_3, 20 % acetonitrile (1-2 mM stocks) and diluted further in 80 mM NH_4HCO_3, 20 % methanol (5-320 μM stocks). VDAC1 peptide was dissolved in 0.1 % acetic acid, 20 % acetonitrile (1-2 mM stocks) and diluted further in 0.1 % acetic acid, 20 % methanol (5-320 μM stocks).

C. Bax preincubation with octylglucoside

Bax (32.4 μM, 0.72 mg/mL) or vehicle (150 mM NaCl, 30 % glycerol, 5 % trehalose, 20 mM TES, pH 7.3, and 2 mM EDTA) was diluted 1:3 in binding buffer (150 mM KCl, 20 mM TES (pH 7.35), 3 mM EDTA, 1 mM DTT, and 0.5% octylglucoside) and incubated on ice for 2-3 hours before use in binding experiments.

D. Equilibrium binding

Triplicate Bax and vehicle samples (1.83 μL) were incubated 60 min, 3·C on an orbital shaker (130 rpm) in binding buffer (180 μL final volume; 110 nM Bax)

supplemented with different concentrations of peptide. Bim or VDAC1 peptide standards

prepared in binding buffer were run in parallel. Samples and standards were transferred to

10 kDa Vivaspin PES filters and centrifuged for 70-90 sec at 12,000 x g at 3 °C. This

typically filtered 40-60% of each sample. Filtrate fluorescence was determined on a

Shimadzu RF6000 spectrofluorophotometer (λ_{ex} = 494 nm, λ_{em} = 524 nm). Fluorescence

of unfiltered standards was also determined to assess the fraction of peptide filtration by

the spin filters.

E. Calculations

The amount of peptide bound was calculated as the difference between the

amount of free peptide in the vehicle and Bax samples.

$$([peptide]_{veh} \times 180) - ([peptide]_{Bax} \times 180) = bound\ peptide\ (fmol)$$

The fraction of peptide standards filtered through the 10 kDa spin filters was

calculated as the ratio of filtered to unfiltered fluorescence.

$$\frac{filtered\ fluorescence}{unfiltered\ fluorescence} = fraction\ filtered$$

F. Blue Native Gel Electrophoresis

Each peptide was diluted in binding buffer to 120 μM and incubated for 2 hr at

3°C on an orbital shaker (130 rpm). Aliquots (10 μL) of each sample were mixed with

blue native loading buffer (3 μL; 100 mM BisTris, pH 7.0, 40 % glycerol) and 5%

Coomassie G250 dye (2 μL). Samples were loaded onto a 3.6% acrylamide stacking and

13-20% acrylamide resolving blue native gel containing 50 mM BisTris, pH 7.0 and 500

mM aminocaproic acid. Samples were run for 100 min at 3 °C between 100-300 volts.

The cathode buffer contained 15 mM BisTris, 50 mM Tricine pH 7.0, and 0.02%

Coomassie G250 dye. The anode buffer contained 50 mM BisTris pH 7.0. Gels were

destained in 40% methanol, 10% acetic acid.

RESULTS

The Bcl-2 homology 3 (BH3) domain has specific amino acids, specifically hydrophobic residues (designated H_0-H_5) and an Asp residue between the H_3 and H_4 position, which characterize this domain. VDAC1 shows a resemblance to this domain with a near identical alignment with the exception of the H_2 position shifted just 1 amino acid closer to the H_1 position. To test the importance of this sequence in the binding of Bax to VDAC1, we mutated these hydrophobic residues in a series of experiments.

Figure 1. Sequence alignments of peptides tested, highlighting BH3 domain and mutations. The Leu at the H_2 position and the Asp between the H_3 and H_4 position are strictly conserved for all BH3 domains. From alignment of the VDAC1 N-terminus with Bim and other BH3 domains (not shown), a similar set of hydrophobic residues (highlighted blue) and a conserved Asp (green) were identified. Specific amino acid substitutions (red) were introduced to test their importance in peptide binding to recombinant Bax.

	K_d (nM)			B_{max} (fmol)			Hill Number		
	1 Site	2 Sites	No Constraint	1 Site	2 Sites	No Constraint	1 Site	2 Sites	No Constraint
VDAC1									
WT	526	1197	1853	19800	39600	57767	1.64	1.41	1.33
H_0H_2 m	626	1677	2798	19800	39600	57381	1.45	1.22	1.15
H_1H_3 m	380	975	2753	19800	39600	82325	1.74	1.37	1.15
H_2H_4 m	461	872	619	19800	39600	32538	1.6	1.6	1.89
H_3H_5 m	389	796	1736	19800	39600	78654	2.17	1.77	1.51
D m	1048	2780	1408	19800	39600	24447	1.34	1.16	1.28
4xE m	1463	5599	1316	19800	39600	18745	1.00	0.83	1.02
Bim									
WT	216	484	3021	19800	39600	204808	1.96	1.60	1.26
H_2 m	928	1408	1101	19800	39600	29561	6	2.42	5.46
4xE m	875	1721	2316	19800	39600	51921	2	2	2

Table 1. Regression results. Calculated dissociation constants (K_D) in nM, maximum bound (B_{max}) in fmol, and hill coefficients for all wild-type and mutant VDAC1 and Bim peptides tested.

Table 1 highlights results from the titrations of all the wild-type and mutant peptides we tested. The dissociation constant (K_D) is a measure of the affinity of the peptide to bind a ligand, specifically Bax in this experiment. The hill coefficient reflects the binding cooperativity between receptor sites. These results were measured through non-linear regression assuming either 1 or 2 binding sites per monomer. The B_{max}, which shows the maximum amount of ligand which the peptide can bind, was calculated from the concentration of recombinant Bax used, assuming either 1 or 2 receptor sites for Bax per monomer.

A. Bax binding to Bim peptides

Bax is an important protein and regulator in the pathway of apoptosis. Bim activates Bax through the binding of its BH3 domain to the hydrophobic groove found in Bax. When Bim activates Bax, Bax oligomerizes at the mitochondrial outer membrane.

9

This allows for the membrane to become permeabilized, which is a key step in apoptosis (Peña-Blanco et al). Bcl-2 family members, such as Bim, are important for binding VDACs, such as VDAC1, in order to regulate the mitochondrial membrane potential and the release of cytochrome c during apoptosis (Shimizu et al. 1999). Because of this, we used the Bim BH3 domain as a positive control to compare Bax binding to VDAC1 peptides.
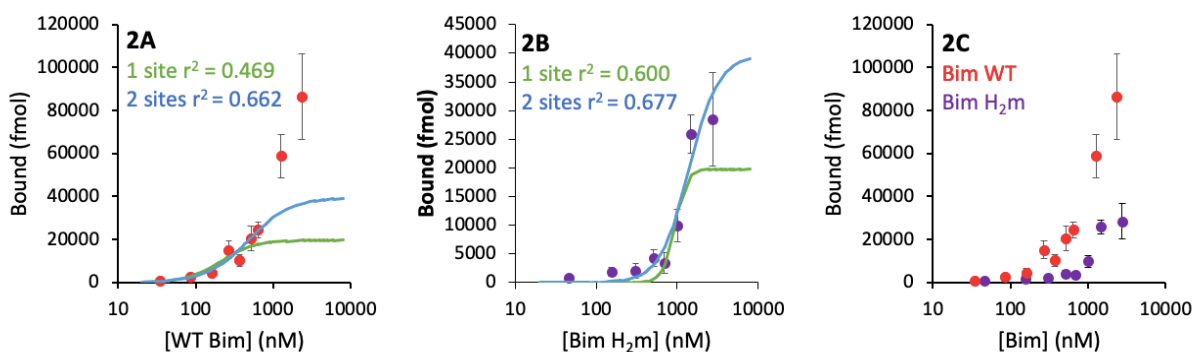

Figure 2. A. Recombinant human Bax binding to wild-type Bim. B. Recombinant human Bax binding to Bim H$_2$m (Leu → Ala). C. Wild-type Bim binding Bax (red) compared to Bim H$_2$m binding Bax (purple). Data are the mean ± SEM of 5-8 experiments. For graphs A and B, non-linear regression curves were fit to the data assuming one binding site per monomer (green, 19800 fmol B$_{max}$) or two sites per monomer (blue, 39600 fmol B$_{max}$). The correlation coefficient for each regression model is color-coded to the corresponding curve.

Bim bound Bax with an affinity ranging from 216-484 nM, depending on if a 1-site or 2-site model was used to determine the K$_D$ by nonlinear regression (Table 1). The nonlinear regression results showed a higher R^2 for the 2-site model, suggesting it could be more fitting and that Bim may have 2 binding sites for Bax (1-site model, R^2= 0.469; 2-site model, R^2=0.662). We utilized the 1-site model and 2-site model, constraining maximum binding to 19,800 fmol or 39,600 fmol respectively, based on reports that Bax has two distinct BH3 domain receptor sites (Gavothiotis et al 2008, Hauseman et al 2020). We were surprised to find that the average amount of peptide bound was higher

than the value expected for 2 sites per monomer. This suggests that either non-specific

binding has occurred or that the stock Bax concentration was higher than reporter by the

manufacturer. For both the 1-site and 2-site model, the hill coefficient exceeded 1.5,

indicating that there could be positive binding cooperativity between binding sites (1-site

model, n_H=1.96; 2-site model, n_H=1.6).

Figure 2B shows the mutation of Leu → Ala at the H_2 position. In the 1-site

model, this resulted in a 4.5-fold loss of affinity of Bax for the Bim peptide, as compared

to the wild-type (H_2m, K_D = 928; WT, K_D = 216). The 2-site model saw similar results,

yielding a 2.9-fold lower affinity of Bax for the Bim H_2m compared to the wild-type

(H_2m, K_D = 1408; WT, K_D = 484). This mutant also showed a hill coefficient higher than

1.5 (1-site model = 6, 2 site model = 2.42) indicating there was positive binding

cooperativity which is consistent with results seen in the wild-type.
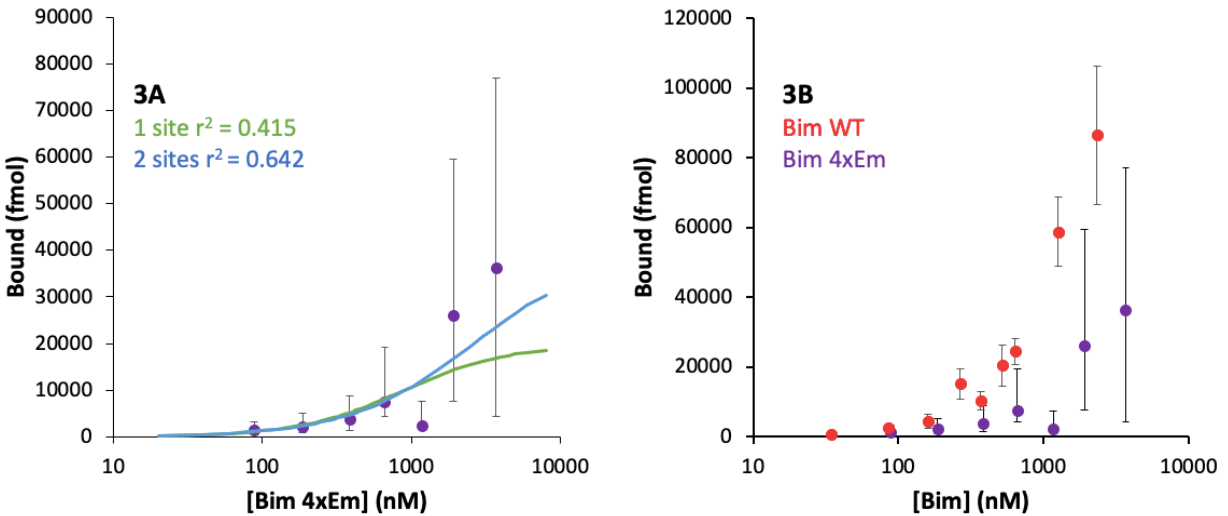
Figure 3. A. Recombinant human Bax binding to Bim 4xEm. B. Wild-type Bim binding Bax (red) compared to Bim 4xEm binding Bax (purple). Data are the mean ± SEM of 5-8 experiments. Non-linear regression curves were fit to the data assuming one binding site per monomer (green, 19800 fmol B_{max}) or two sites per monomer (blue, 39600 fmol B_{max}). The correlation coefficient for each regression model is color-coded to the corresponding curve.

For the Bim 4xE mutant, the residues at the positions H_1-H_4 were mutated. The mutation caused a decrease in affinity of Bax for the peptide by 4-fold for the 1-site model ($K_D = 875$) and 3.6 fold for the 2-site model ($K_D = 1721$) compared to wild-type Bim. This mirrors the results from the H_2m mutation with a similar decrease in affinity upon mutation. Similar to the WT and H_2m, both models of the Bim 4xEm show a hill coefficient higher than 1.5, which is indicative of positive cooperativity among binding sites (1-site model = 2.0, 2-site model = 2.0).

B. Bax binding VDAC1

Voltage dependent anion channel 1 (VDAC1) is located in the mitochondrial outer membrane (MOM) and could potentially interact with Bax located around the mitochondria. We titrated VDAC1 to determine if the proposed BH3-like domain behaves and binds in the same way as a known BH3 domain (Bim). If so, our goal was to determine which residues were most important in binding.
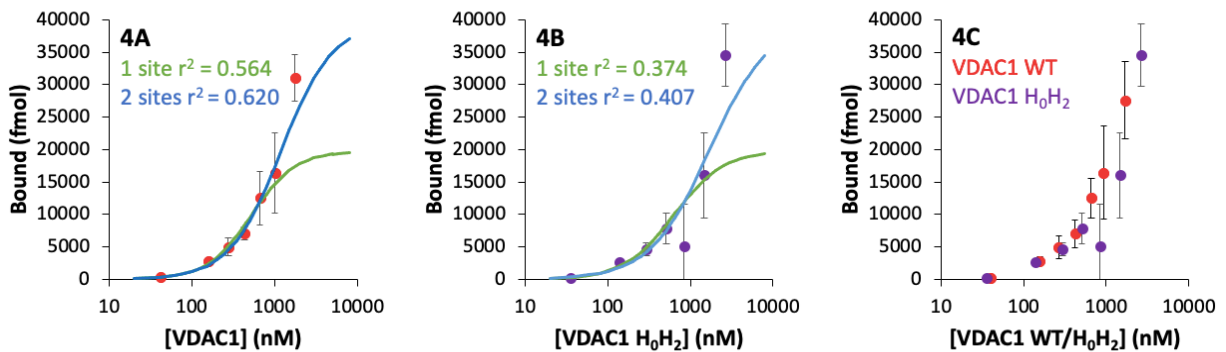
Figure 4. A. Recombinant human Bax binding to wild-type VDAC1. B. Recombinant human Bax binding to VDAC1 H_0H_2m. C. Wild-type Bim binding Bax (red) compared to VDAC1 H_0H_2m binding Bax (purple). Data are the mean ± SEM of 5-8 experiments. For graphs A and B, non-linear regression curves were fit to the data assuming one binding site per monomer (green, 19800 fmol B_{max}) or two sites per monomer (blue, 39600 fmol B_{max}). The correlation coefficient for each regression model is color-coded to the corresponding curve.

Wild-type VDAC1 bound Bax with a 2.4 lower affinity than the known BH3 domain (Bim) did in the 1-site model (VDAC1, $K_D = 526$; Bim, $K_D = 216$). In the 2-site

model, VDAC1 bound Bax with a 2.5 lower affinity than Bim (VDAC1, K_D = 1197; Bim, K_D = 484). For the WT VDAC1, the 2-site model was a better fit than the 1-site model indicating that similar to Bim, VDAC1 may have two binding sites (1-site, R^2 = 0.564; 2-site, R^2 = 0.620). The hill coefficient for WT VDAC1 was around 1.5 for both the 1-site and 2-site model, indicating that there may be positive binding cooperativity among binding sites (1-site model, n_H=1.64; 2-site model, n_H=1.41).

The VDAC1 H_0H_2 mutant was mutated at the H_0 position from Pro to Gly and the H_2 position from Leu to Ala. The VDAC1 H_0H_2 mutant bound Bax with a slightly lower affinity (1.2-fold) compared to the WT VDAC1 in the 1-site model, and a 1.4-fold lower affinity in the 2-site model (1-site model, K_D= 626; 2-site model, K_D= 1677). This mutant, which altered the H_2 position, did not show as much of a decrease in binding affinity (1 site = 1.2-fold, 2 site = 1.4-fold) when it is compared to the WT as the Bim H_2 mutant (1 site = 4.5 fold, 2 site = 2.9 fold) showed. This could indicate that the residue at the H_2 position in VDAC1 is not as important for binding as the residue at the H_2 position is for a known BH3 domain.

For the H_0H_2 mutant, the 2-site model was a slightly better fit than the 1-site model (1-site, R^2 = 0.374; 2-site, R^2 = 0.407) which is consistent with previous mutants. The hill number for the 1-site could be indicative of positive cooperativity among binding sites, but the 2-site model does not support this (1-site model, n_H=1.45; 2-site model, n_H=1.22).

Figure 5. A. Recombinant human Bax binding to VDAC1 H_1H_3 m. Non-linear regression curves were fit to the data assuming one binding site per monomer (green, 19800 fmol B_{max}) or two sites per monomer (blue, 39600 fmol B_{max}). The correlation coefficient for each regression model is color-coded to the corresponding curve. B. Wild-type Bim binding Bax (red) compared to VDAC1 H_1H_3m binding Bax (purple).

The VDAC1 H_1H_3 mutant showed a slight increase in binding affinity to Bax upon mutation of the H_1 and H_3 residues for both the 1-site and 2-site models (1-site model, K_D= 380; 2-site model, K_D= 975) compared to WT VDAC1, with a 1.4-fold increase in affinity in the 1-site model and a 1.2-fold increase in the 2-site model. The 2-site model once again shows a better fit to the data (1-site, R^2 = 0.427; 2-site, R^2 = 0.498). In regard to positive binding cooperativity, the 1-site model indicates it could be present, while the 2-site model does not necessarily support positive binding cooperativity (1-site model, n_H=1.74; 2-site model, n_H=1.37).
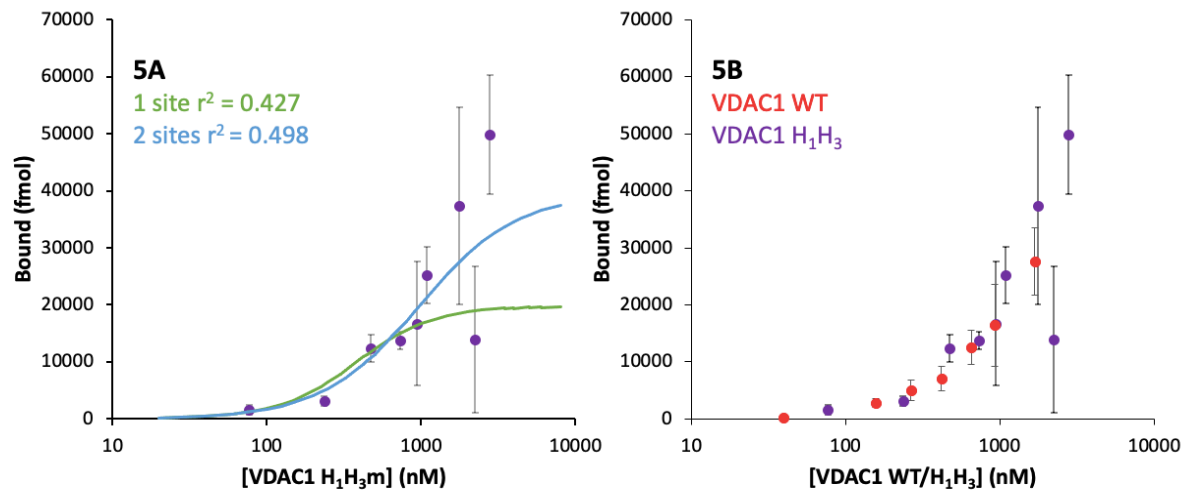
14

Figure 6. A. Recombinant human Bax binding to VDAC1 H_2H_4 m. Non-linear regression curves were fit to the data assuming one binding site per monomer (green, 19800 fmol B_{max}) or two sites per monomer (blue, 39600 fmol B_{max}). The correlation coefficient for each regression model is color-coded to the corresponding curve. B. Wild-type Bim binding Bax (red) compared to VDAC1 H_2H_4m binding Bax (purple).

The VDAC1 H_2H_4 mutant has the Leu at the H_2 position mutated to a Ala, and the Phe at the H_4 position mutated to a Gly. The VDAC1 H_2H_4 mutant, similar to the VDAC1 H_1H_3 mutant, showed an increase in binding affinity (1-site model, K_D= 461; 2-site model, K_D= 872) for both the 1-site (1.1 fold) and 2-site (1.4 fold) models compared to the WT VDAC1. The VDAC1 H_0H_2 mutation did cause a slight decrease in binding affinity, which cannot be seen in the VDAC1 H_2H_4 mutant which also altered the H_2 position.

Both the 1-site model and the 2-site model show similar correlation coefficients, indicating that they are similar in their goodness of fit to the data (1-site, $R^2 = 0.452$; 2-site, $R^2 = 0.453$). They also have the same hill number (n_H=6) for the 1-site and 2-site model, indicating that positive binding cooperativity could be present.
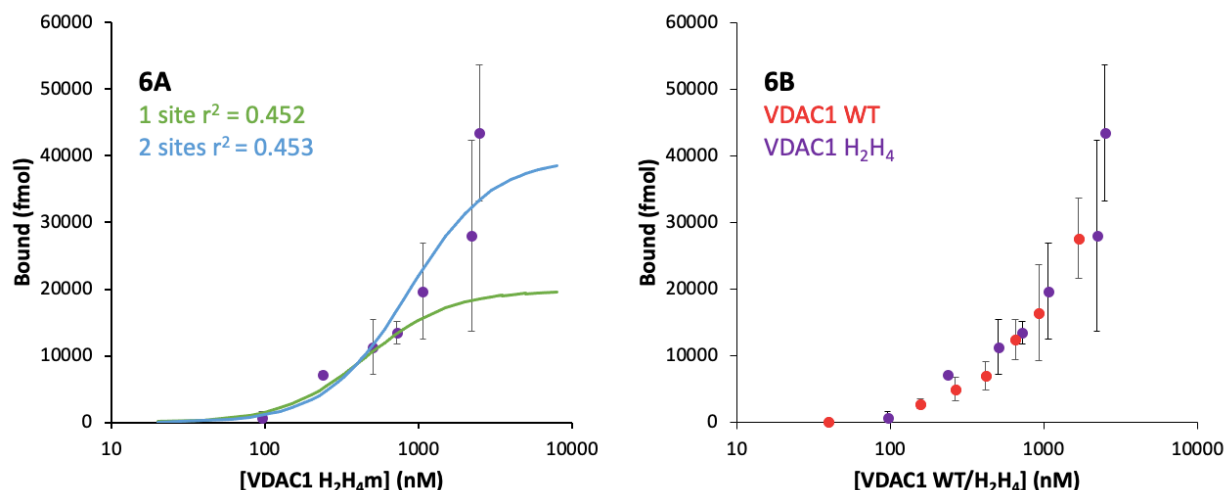
Figure 7. A. Recombinant human Bax binding to VDAC1 H_3H_5m. Non-linear regression curves were fit to the data assuming one binding site per monomer (green, 19800 fmol B_{max}) or two sites per monomer (blue, 39600 fmol B_{max}). The correlation coefficient for each regression model is color-coded to the corresponding curve. B. Wild-type Bim binding Bax (red) compared to VDAC1 H_3H_5m binding Bax (purple).

The VDAC1 H_3H_5 mutant has the Ala at the H_3 position mutated to Gly, and the Tyr at the H_5 position mutated to Ala. The VDAC1 H_3H_5 mutant again showed an increase in binding affinity (1-site model, K_D= 389; 2-site model, K_D= 796) compared to the WT VDAC1. There was a 1.4-fold increase in binding affinity in the 1-site model and a 1.5-fold increase in binding affinity in the 2-site model, compared to the WT VDAC1. This mutation at the H_3 position in the H_1H_3 mutant also showed an increase in binding affinity.

The 2-site model was the better fit for the data, indicating that there may be 2 binding sites present (1-site, $R^2 = 0.327$; 2-site, $R^2 = 0.427$). Both models showed hill numbers above 1.5, indicating that there could be positive cooperativity among binding sites (1-site model, n_H=2.17; 2-site model, n_H=1.77).
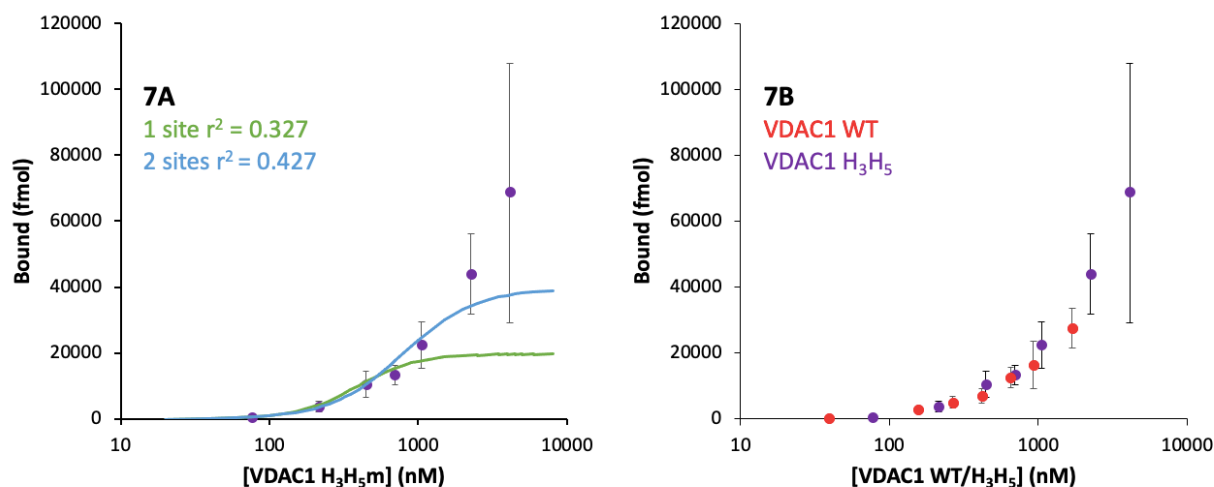
Figure 8. A. Recombinant human Bax binding to VDAC1 Dm (Asp -> Arg). Non-linear regression curves were fit to the data assuming one binding site per monomer (green, 19800 fmol B_{max}) or two sites per monomer (blue, 39600 fmol B_{max}). The correlation coefficient for each regression model is color-coded to the corresponding curve. B. Wild-type Bim binding Bax (red) compared to VDAC1 Dm binding Bax (purple).

The VDAC1 D mutant has the Asp residue between the H_3 and H_4 position mutated to Arg. The VDAC1 D mutant showed a decrease in binding affinity compared to WT VDAC1 (1-site model, K_D= 1048; 2-site model, K_D= 2780). This is a 2-fold decrease in affinity from the WT VDAC1 for the 1-site model and a 2.3-fold decrease in affinity for the 2-site model. This decrease in affinity supports the possibility that the Asp residue is important for binding VDAC1 to Bax.

For this mutant, the 2-site model is a better fit to the data (1-site, R^2 = 0.500; 2-site, R^2 = 0.542). Both hill numbers are below 1.5, but above 1. This does not necessarily support positive binding cooperativity (1-site model, n_H=1.34; 2-site model, n_H=1.16).

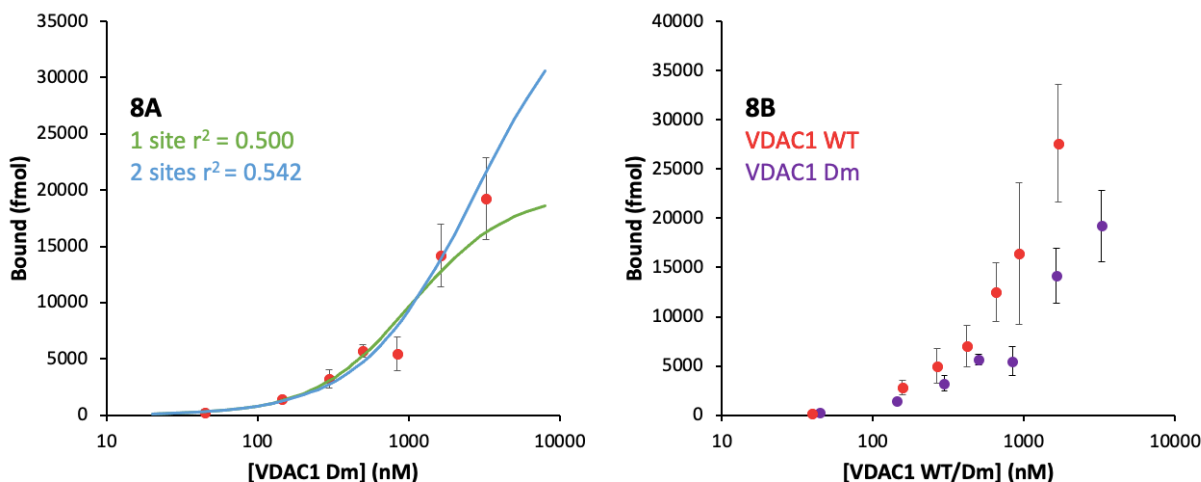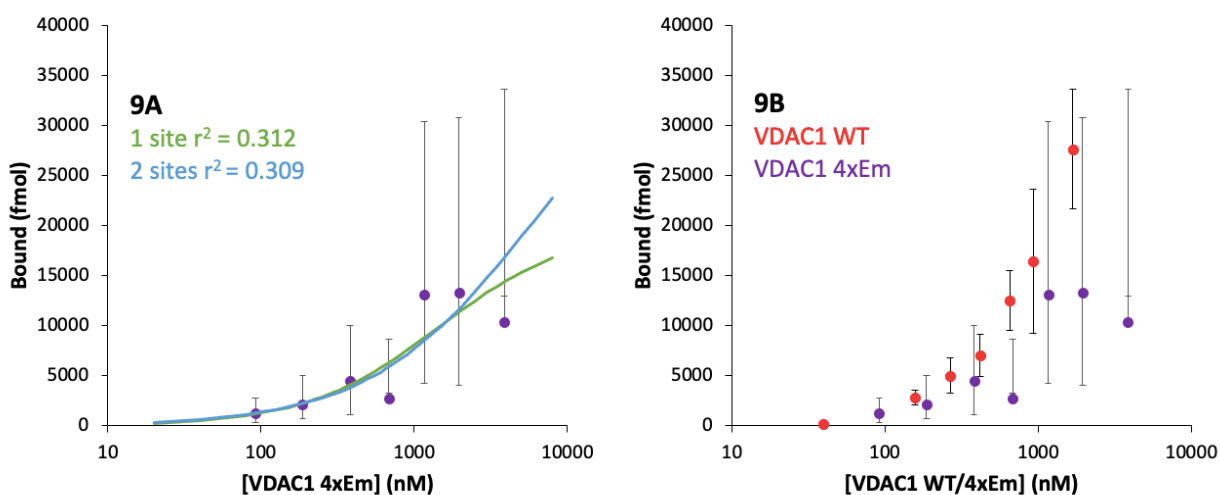*Figure 9. A. Recombinant human Bax binding to VDAC1 4xEm. Non-linear regression curves were fit to the data assuming one binding site per monomer (green, 19800 fmol B_{max}) or two sites per monomer (blue, 39600 fmol B_{max}). The correlation coefficient for each regression model is color-coded to the corresponding curve. B. Wild-type Bim binding Bax (red) compared to VDAC1 4xEm binding Bax (purple).*

The VDAC1 4xE mutant was mutated so that the residues at the H_1-H_4 position were changed to glutamate. The VDAC1 4xE mutant showed a strong decrease in affinity for the Bax peptide compared to the WT VDAC1 (1-site model, K_D= 1463; 2-site model, K_D= 5599). Compared to WT VDAC1, VDAC1 4xE had a 2.8-fold lower affinity for Bax in the 1-site model and a 4.7-fold lower affinity for Bax in the 2-site model. This mutant had the largest decrease in affinity of all the mutant VDAC1 peptides, suggesting that the mutation caused a large disruption in binding. It's interesting to see that only 1 double mutant out of 4 caused a decrease in binding affinity (H_1H_3), but the combination of 4 (H_1-H_4) caused a large decrease in binding affinity. This could be due to the fact that the VDAC1 4xE mutant altered all the residues to glutamate, instead of alanine and glycine like the double mutants.

Both the 1-site model and the 2-site model yielded similar correlation coefficients (1-site, $R^2 = 0.312$; 2-site, $R^2 = 0.309$), seemingly suggesting they are both equally good models. VDAC1 4xE also yielded the lowest hill numbers (1-site model, n_H=1.00; 2-site

18

model, n_H=0.83). This mutant seems to present less positive binding cooperativity than other mutants.

Figure 10. A. VDAC1 Peptide Filtration results. WT and mutant VDAC1 peptides were filtered through a 10 kDa spin filter and results show the amount of VDAC1 which filtered through the spin filter. B. Gel Electrophoresis. The relative sizes of WT and mutant VDAC1 peptides on blue native gel. Sizes were estimated based on standards (left and right).

C. VDAC1 Peptide Filtration and Gel Electrophoresis

Further analysis showed that most VDAC1 peptides were not being filtered through the 10 kDa spin filters during centrifugation. The VDAC1 4xE mutant showed the highest amount filtered. All double mutants were less than 10 percent filtered through, with the exception of the H_2H_4 mutant, which had around 30% filtered. We expected the VDAC1 peptide to be well under 10 kDa, but gel electrophoresis showed that most peptides were weighing in between 6.5-14.8. These results could show that wild-type and mutant VDAC1 peptides were forming dimers, trimers, and other oligomers, preventing predicted peptide filtration. The gel electrophoresis also showed the VDAC1 4xE mutant to have a strong band around 3.2 kDa, supporting our results of its high filtration through a 10 kDa spin filter.

11A

11B

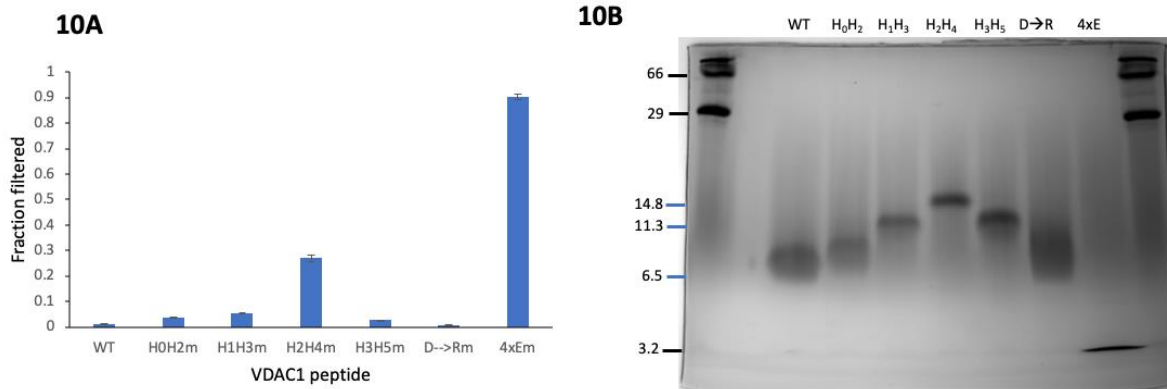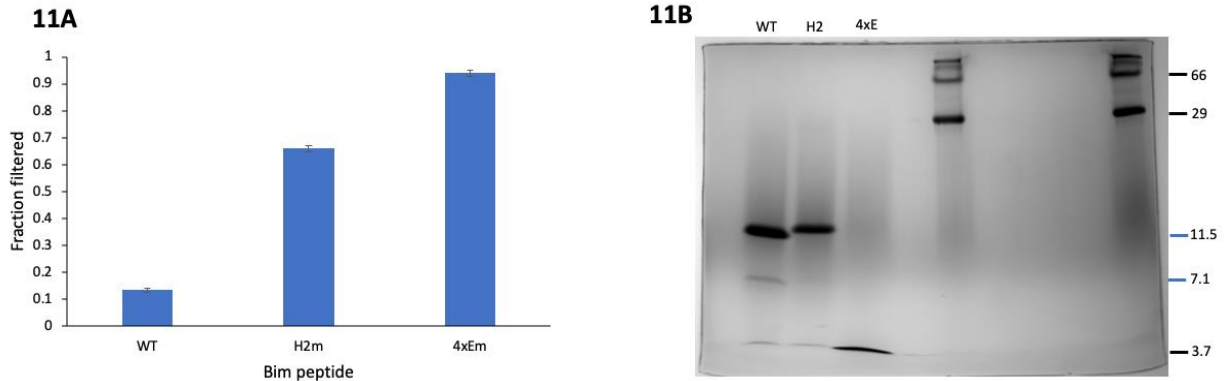*Figure 11. A. Bim Peptide Filtration results. WT and mutant Bim peptides were filtered through a 10 kDa spin filter and results show the amount of Bim which filtered through the spin filter. B. Gel Electrophoresis. The relative sizes of WT and mutant Bim peptides on blue native gel. Sizes were estimated based on standards (left and right).*

D. Bim Filtration and Gel Electrophoresis

Wild-type Bim showed the lowest amount filtered (~12%). The mutant H_2m and

4xE m peptides showed much higher filtration (~67% and 95%). Wild-type Bim and the

H_2 mutant showed a very strong band around 11.5 kDa, while the 4xE mutant showed the

strongest band around 3.7 kDa. The 4xE mutant showed the lowest molecular weight

which reaffirms that it had the highest filtration through a 10 kDa spin filter.

DISCUSSION

The important findings from the current study are that (a) recombinant Bax binds to a synthetic peptide corresponding to the N-terminus of VDAC1, (b) binding involved hydrophobic residues and a conserved Asp in VDAC1 consistent with known BH3 domains, (c) Bax has a lower affinity for the VDAC1 BH3-like domain than the Bim BH3 domain, possibly because of the position shift in the conserved H_2 Leu together with the larger hydrophobic residues at H_1 and H_5 creating steric hindrance within the groove, and (d) the stoichiometry of binding suggests that Bax contains two receptor sites for both the VDAC1 and Bim BH3 domains. These data support the hypothesis that VDAC1 is a novel member of the Bcl-2 family involved in regulating Bax, and potentially other Bcl-2 family members, through its N-terminal BH3 domain. Further experiments are necessary to determine if the VDAC1 BH3 domain is involved in activating or sequestering Bax, and the physiological conditions which may trigger movement of the BH3 domain from the protected VDAC1 pore to the cytoplasmic environment such that binding to Bax or other Bcl-2 family members can occur.

Monomeric, inactive Bax has nine alpha helices (α1-α9), with its central hydrophobic helix (α5) located in the center of the molecule (Westphal et al, 2013). The BH3 domain is located within the 2nd alpha helix (α2) and is unavailable to bind other Bcl-2 family members, including other Bax monomers, when Bax is inactive. The 9th helix (α9) is sequestered in a hydrophobic groove formed by $α2$-$α5$ in inactive Bax, but is thought to become a transmembrane domain which anchors the active protein in the MOM. (Westphal et al 2013). When $α9$ is displaced from the hydrophobic groove by a conformational change that may involve an activator BH3 domain (Hauseman et al

21

2020), the unoccupied groove becomes the canonical binding site for at least some BH3

domains. The hydrophobic residues in the BH3 domain interact with multiple

hydrophobic residues within the groove and the conserved Asp between H_3 and H_4 forms

a critical salt bridge with α4 Arg107 in the groove. Some BH3 domain-hydrophobic

groove interactions (e.g., with Bim and others that have activator BH3 domains)

destabilize Bax's tertiary structure in a way that results in exposure of the Bax BH3

domain and subsequent formation of Bax dimers and higher molecular weight oligomers

(Czabotar et al 2013) that ultimately cause cytochrome c release. In contrast, other BH3

domain-groove interactions (e.g., with Bad and others that have sensitizer or pro-survival

BH3 domains) do not affect Bax conformation, which prevents oligomerization and

cytochrome c release. One important finding from the current study is that Bax likely has

2 BH3 domain binding sites per monomer, as the 2-site model consistently gave higher

correlation coefficients compared to the 1-site model (Figs. 2-9). Bax has one widely

agreed upon binding site found in the hydrophobic groove of the protein, but a

hypothetical second binding site has not been extensively studied. In 2008, Gavathiotis et

al was the first to identify and describe a second, distinct BH3 domain binding site,

composed of residues in α1 and α6, on Bax (Gavathiotis et al 2008). Our findings do not

isolate a location of a second binding site, but they support the existence of a second BH3

binding site on Bax. Recent evidence suggests that BH3 domain binding to this 'non-

canonical' site may be the trigger that releases α9 from the hydrophobic groove to direct

Bax insertion into the MOM prior to activator-induced oligomerization (Dengler et al

2019). Since the non-canonical site structurally differs from the hydrophobic groove, the

affinity of each site is likely to differ for any given BH3 domain. Thus, while the current

binding stoichiometry results support 2 discrete binding sites, the data are insufficient to resolve site-specific affinities, so the 2-site K_D value reported for each peptide is likely an average of the affinities from both sites; each KD should thus be considered an apparent rather than true affinity. This complicates interpretation of Bax affinity for each mutant, as the affinity of each site for a given mutant may vary in different ways.

We found that the H_1-H_4 hydrophobic residues in the VDAC1 domain have a similar role in establishing affinity for Bax as in the Bid BH3 domain, as demonstrated by the impact of the quadruple non-conservative (4xE) mutant on binding (Fig. 1). Introduction of four negatively charged Glu for H_1-H_4 residues resulted in a 3.6-fold lower binding affinity of Bax for Bim compared to a 4.7-fold lower binding affinity for VDAC1. A substantial decrease in binding affinity was observed for both the known BH3 domain of Bim and the proposed BH3 domain of VDAC1. We propose that the lower affinity is the result of the charged glutamate impeding binding to the hydrophobic groove in Bax. This leads us to conclude that the H_1-H_4 hydrophobic residues are important for Bax binding VDAC1, similar to the role of these residues in known BH3 domains facilitating binding to Bax (Czabotar et al 2013, Westphal et al 2014). Previous studies have also shown that mutagenesis of a known BH3 domain, specifically the hydrophobic face of the BH3 domain and charged residues, had great effect on the binding activity and death agonist activity (Wang et al 1998). This aligns with our results, both in regard to Bim and VDAC1.

Another conserved feature of all BH3 domains is an Asp residue between the H_3 and H_4 positions (Fig 1). Prior studies have shown that this residue is important for binding of BH3 domains to the Bax hydrophobic groove. A study found that the

conserved Asp residue is a crucial site within the BH3 domain of BAD for the interaction

of BAD with Bcl-2 (Adachi et al 2002). Another study found that a D68R mutant,

mutation of the Asp residue to Arg in the BH3 activator domain of Bim, was not able to

dimerize and activate Bax (Czabotar et al 2013). These both show the importance of the

Asp residue within the BH3 domain in regard to binding. Similar to known BH3

domains, VDAC1 also has an Asp residue found between the H_3 and H_4 positions. To test

the significance of this Asp residue within VDAC1, we mutated the Asp residue to Arg.

We found a 2.3-fold loss of affinity of this VDAC1 mutant for Bax compared to VDAC1

WT. This confirms that this Asp residue is important for binding VDAC1 to Bax, in the

same way that this residue is important for Bax binding to known BH3 domains. This

further supports our idea that VDAC1 binds in a similar manner as known BH3 domains.

Computational analysis revealed that this Asp residue is proposed to form a salt bridge

with Arg 107 within the Bax hydrophobic groove as with Bim (Pandey et al, in

preparation). At a neutral pH, Asp is negatively charged. By altering this residue to Arg,

we have generated a negative to positive charge swap. If this proposed interaction is

correct, the Asp -> Arg mutation would create charge repulsion with the Arg 107 found

within the Bax hydrophobic groove. This explains the reduced affinity at the hydrophobic

groove site, but could also negatively affect the affinity at the $\alpha1/\alpha6$ site, as the Asp in

Bim is proposed to form a salt bridge with Arg134 in Bax (Gavathiotis et al 2008,

Dengler 2019).

Since the non-conservative quadruple substitutions of H_1-H_4 with glutamates

resulted in substantial reduction in Bax affinity for VDAC1, we performed more

conservative double point mutations on the hydrophobic residues in the VDAC1 domain

to further test their importance. The H_0H_2 mutant with Pro $\rightarrow$ Gly mutation at the H_0 (+1) position, shifted one residue towards the H_1 position, and a Leu $\rightarrow$ Ala mutation at the H_2 position of VDAC1 (Fig. 1) was the only double mutant having a lower (1.4-fold) affinity for Bax. It is possible that both substitutions contribute to the lower affinity, or that the two changes have opposite effects, but with the one causing lower affinity dominating. In this regard, it is worth noting that the VDAC1 H_2 position, which is a strictly conserved Leu in all Bcl-2 family members that is important for binding (Czabotar et al 2013), is shifted one residue towards H_1, in comparison to the Bim (and other Bcl-2 family members) BH3 domain (Fig. 1). Our results confirm that the Bim H_2 Leu is an important contributor to binding Bax, as the single H_2 Leu$\rightarrow$Ala mutant exhibited a 2.9-fold lower affinity. The non-conserved positioning of H_2 Leu in VDAC1 may change the position of it within the α-helix and thus hydrophobic groove such that it has a smaller (or negative) contribution to driving affinity for Bax. Computational docking analysis of VDAC1 peptide in the Bax hydrophobic groove predicts that the one-residue shift toward H_1 results in H_2 Leu and H_1 Tyr, which have relatively large side chains, making hydrophobic contact with the same Bax Met79 residue (Pandey et al, manuscript in preparation). In contrast, Bim H_2 interacts with Met99 and Phe116 in Bax while the H_1 Ile interacts with Met79 (Czabotar et al 2013). This raises the possibility of H_1/H_2 steric constraints in VDAC1 with Met79 that do not occur with known BH3 domains. From this, we speculate that the H_2 change from a relatively large Leu to a smaller hydrophobic Ala in the H_0H_2 mutant may relieve such constraints while still contributing to the hydrophobic interaction with Bax, and thus drive increased affinity. This implies that Pro$\rightarrow$Gly swap at H_0 (+1) is therefore the critical change driving the lower affinity.

Experiments with the VDAC1 H_0 (+1) point mutant Pro→ Gly are necessary to test the importance of this residue.

Further evidence on the role of Pro at H_0 (+1) can be gained from comparison of H_0H_2 and H_2H_4 mutant affinities. In contrast to this mutant, the H_2H_4 Leu→Ala and Phe→Gly substitutions surprisingly resulted in a 1.5-fold increase in affinity. Bax thus exhibits a 2-fold higher affinity for H_2H_4 vs. H_0H_2 mutant. Since both peptides share the same H_2 Leu→Ala swap, the higher affinity for the H_2H_4 mutant is the result of the native H_0 (+1) Pro (vs. Gly) and/or the Gly substituted at H_4 (vs. the native Phe). We propose that the Pro at H_0 (+1) is important to the higher affinity, given that computational docking studies predict hydrophobic interactions of this Pro with Val91 and Val95 of Bax (Pandey et al, manuscript in preparation). Furthermore, previous studies have shown the two Ile at H_0 in Bid are important for activating Bax. Mutation of both amino acids at the H_0 sequence to two alanines found a decrease in ability to release cytochrome c, indicating that binding and activation was inhibited (Czabotar et al 2013). Whether the H_4 substitution Phe→Gly in the H_2H_4 mutant contributes to its higher affinity for Bax is unknown, but we speculate that glycine at this position is more likely to negatively affect Bax affinity given that this is a small, polar residue. Thus, computational docking and experimental evidence indicate the second proline at the H_0 (+1) position is important in promoting Bax affinity for the wild type VDAC1 peptide.

For the VDAC1 H_1H_3 mutant, the H_1 Tyr → Ala and the H_3 Ala → Gly substitutions (Fig. 1) resulted in a modest 1.2-fold increase in affinity for Bax. By the same steric hindrance rationale proposed earlier for the non-conserved position of H_2 Leu, the substitution of a large tyrosine for a small hydrophobic alanine is predicted to

26

relieve H_1/H_2 steric constraints with Met79 in Bax and thus promote higher affinity. In contrast, we propose that the H_3 Ala→Gly substitution promotes a decrease in affinity for Bax. Computational docking studies predict that the H_3 Ala in VDAC1 interacts with Leu 70 of Bax (Pandey et al, manuscript in preparation). Upon mutation of Ala → Gly, this position loses its hydrophobic character which would decrease the ability of the H_3 position to interact with Leu 70 in Bax. The increase in affinity driven by the H_1 change is proposed to be marginally greater than the decrease in affinity from the H_3 change, resulting in a smaller KD value, reflecting a 1.2-fold higher affinity.

Finally, Bax exhibited a 1.5-fold higher affinity compared to wild type VDAC1 for the H_3H_5 mutant that consisted of an Ala → Gly mutation at H_3 and a Tyr → Ala mutation at H_5. This mutant has the same H_3 substitution as the H_1H_3 mutant, which we suggest would cause a decrease in affinity of Bax for the peptide due to losing the hydrophobic character of the H_3 position. By extension, this implies that the increase in affinity for this peptide is due to the H_5 substitution of the large tyrosine having both hydrophobic and polar properties for the small hydrophobic alanine. Other studies have found that H_5 of the Bim peptide sits at the periphery of the hydrophobic groove and has little interaction with Bax residues as homo-oligomerization still occurred upon mutation of this residue site (Czabotar et al 2013). This group hypothesized that the H_5 position may be outside of the dimerization interface (Czabotar et al 2013). However, computational docking studies found that the H_5 Tyr in VDAC1 is proposed to form contacts with Val 111 and Phe 165 in Bax (Pandey et al, in preparation). Both Val and Phe are hydrophobic residues which would potentially interact with Tyr through hydrophobic interactions, but the convergence of the three larger residues could create

steric constraints that are relieved by the smaller Ala. This would increase VDAC1

H_3H_5's ability to bind the hydrophobic groove of Bax, and specifically Val 111 or Phe

165. We propose that the increase in affinity of Bax for VDAC1 H_3H_5 compared to

VDAC1 WT is from the mutation at the H_5 position. Since Bax exhibited a higher affinity

for the H_3H_5 than the H_1H_3 mutant, relieving the steric constraint at H_5 by substitution

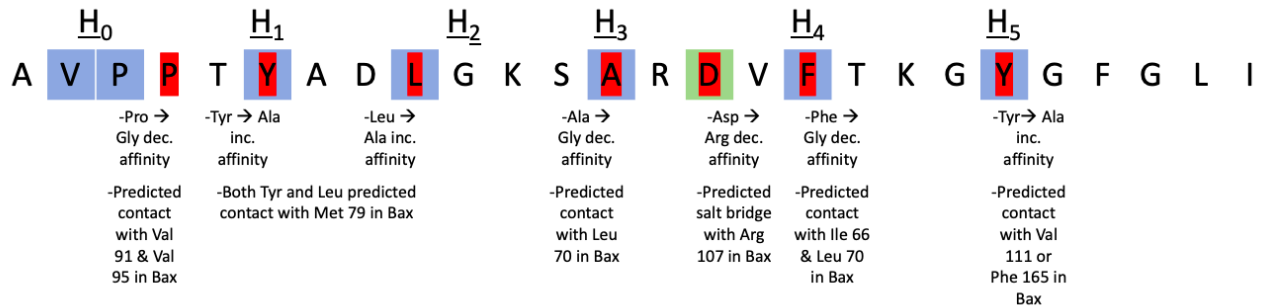with alanine appears to be more important than a similar change at the H_1 position. .

Figure 12. Summary of findings regarding VDAC1. The proposed BH3 domain of VDAC1 is listed. The hydrophobic domain (H_0-H_5) is highlighted in blue, the conserved asp residue in green, and the residue mutated in red.

CONCLUSION

In conclusion, we found evidence that the N-terminus of VDAC1 binds Bax in a way that is consistent with known BH3 domains. The conserved aspartate between H_3 and H_4 is important for the interaction, as is the proline at H_0+1, as predicted from computational docking studies. The one-position change in the strictly conserved Leu at H_2 is a notable difference that likely negatively affects the affinity for VDAC1 vs. Bim peptide. The shift one residue toward H_1 potentially creates steric constraints with the H_1 tyrosine, both of which are predicted to interact with the same methionine in Bax. Tyrosine H_5 may have a more influential role in VDAC1 than Bim because of how the peptide is predicted to dock in the hydrophobic groove, creating steric constraints similar to H_1/H_2 that may contribute to lowering Bax affinity for VDAC1. Since non-conservative mutation of all four hydrophobic residues (H_1-H_4) to glutamates (table 1) substantially reduced affinity for VDAC1, these residues collectively are important for binding just as they are known to be important in known BH3 domains. Further experiments are necessary to determine if the VDAC1 BH3 domain destabilizes inactive Bax to promote activation or prevents activation by stabilizing the inactive conformation.

REFERENCES

1. Siddiqui, Manzer H et al. "Morphological and physiological characterization of different genotypes of faba bean under heat stress." *Saudi journal of biological sciences* vol. 22,5 (2015): 656-63. doi:10.1016/j.sjbs.2015.06.002

2. Warren, Chloe FA, Michelle W. Wong-Brown, and Nikola A. Bowden. "BCL-2 family isoforms in apoptosis and cancer." *Cell death & disease* 10.3 (2019): 177.

3. Kale, Justin, Elizabeth J. Osterlund, and David W. Andrews. "BCL-2 family proteins: changing partners in the dance towards death." *Cell Death & Differentiation* 25.1 (2018): 65-80.

4. Lomonosova, Elena, and G. Chinnadurai. "BH3-only proteins in apoptosis and beyond: an overview." *Oncogene* 27.1 (2008): S2-S19.

5. Birkinshaw, Richard W., and Peter E. Czabotar. "The BCL-2 family of proteins and mitochondrial outer membrane permeabilisation." *Seminars in cell & developmental biology*. Vol. 72. Academic Press, 2017.

6. Green, Douglas R. "Apoptotic pathways: ten minutes to dead." *Cell* 121.5 (2005): 671-674.

7. Adams, Jerry M., and Suzanne Cory. "The Bcl-2 protein family: arbiters of cell survival." *Science* 281.5381 (1998): 1322-1326.

8. Kale, Justin, Elizabeth J. Osterlund, and David W. Andrews. "BCL-2 family proteins: changing partners in the dance towards death." *Cell Death & Differentiation* 25.1 (2018): 65-80.

9. Hsu, Yi-Te, and Richard J. Youle. "Bax in murine thymus is a soluble monomeric protein that displays differential detergent-induced conformations." *Journal of Biological Chemistry* 273.17 (1998): 10777-10783.

10. Hsu, Yi-Te, Keith G. Wolter, and Richard J. Youle. "Cytosol-to-membrane redistribution of Bax and Bcl-XL during apoptosis." *Proceedings of the National Academy of Sciences* 94.8 (1997): 3668-3672.

11. Renault, Thibaud T., and Stéphen Manon. "Bax: Addressed to kill." *Biochimie* 93.9 (2011): 1379-1391.

12. Wolter, Keith G., et al. "Movement of Bax from the cytosol to mitochondria during apoptosis." *The Journal of cell biology* 139.5 (1997): 1281-1292.

13. Guedes, Joana P., et al. "Acetic acid triggers cytochrome c release in yeast heterologously expressing human Bax." *Apoptosis* 27.5-6 (2022): 368-381.

14. Lalier, Lisenn, et al. "Bax activation and mitochondrial insertion during apoptosis." *Apoptosis* 12 (2007): 887-896.

15. Shoshan-Barmatz, Varda, Anna Shteinfer-Kuzmine, and Ankit Verma. "VDAC1 at the intersection of cell metabolism, apoptosis, and diseases." *Biomolecules* 10.11 (2020): 1485.

16. Bayrhuber, Monika, et al. "Structure of the human voltage-dependent anion channel." *Proceedings of the National Academy of Sciences* 105.40 (2008): 15370-15375.

17. Hiller, Sebastian, et al. "Solution structure of the integral human membrane protein VDAC-1 in detergent micelles." *Science* 321.5893 (2008): 1206-1210.

18. Ujwal, Rachna, et al. "The crystal structure of mouse VDAC1 at 2.3 Å resolution reveals mechanistic insights into metabolite gating." *Proceedings of the National Academy of Sciences* 105.46 (2008): 17742-17747.

19. Hiller, Sebastian, and Gerhard Wagner. "The role of solution NMR in the structure determinations of VDAC-1 and other membrane proteins." *Current opinion in structural biology* 19.4 (2009): 396-401.

20. Geula, Shay, Danya Ben-Hail, and Varda Shoshan-Barmatz. "Structure-based analysis of VDAC1: N-terminus location, translocation, channel gating and association with anti-apoptotic proteins." *Biochemical Journal* 444.3 (2012): 475-485.

21. Abu-Hamad, Salah, et al. "The VDAC1 N-terminus is essential both for apoptosis and the protective effect of anti-apoptotic proteins." *Journal of cell science* 122.11 (2009): 1906-1916.

22. Shi, Yong, et al. "Identification of the protein–protein contact site and interaction mode of human VDAC1 with Bcl-2 family proteins." *Biochemical and biophysical research communications* 305.4 (2003): 989-996.

23. Arbel, Nir, Danya Ben-Hail, and Varda Shoshan-Barmatz. "Mediation of the antiapoptotic activity of Bcl-xL protein upon interaction with VDAC1 protein." *Journal of Biological Chemistry* 287.27 (2012): 23152-23161.

24. Arzoine, Laetitia, et al. "Voltage-dependent anion channel 1-based peptides interact with hexokinase to prevent its anti-apoptotic activity." *Journal of Biological Chemistry* 284.6 (2009): 3946-3955.

25. Camara, Amadou KS, Martin Bienengraeber, and David F. Stowe. "Mitochondrial approaches to protect against cardiac ischemia and reperfusion injury." *Frontiers in physiology* 2 (2011): 13.

26. Camara, Amadou KS, Edward J. Lesnefsky, and David F. Stowe. "Potential therapeutic benefits of strategies directed to mitochondria." *Antioxidants & redox signaling* 13.3 (2010): 279-347.

27. Shimizu, Shigeomi, et al. "Bcl-2 family proteins regulate the release of apoptogenic cytochrome c by the mitochondrial channel VDAC." *Nature* 399.6735 (1999): 483-487.

28. Gavathiotis, Evripidis, et al. "BAX activation is initiated at a novel interaction site." *Nature* 455.7216 (2008): 1076-1081.

29. Hauseman, Zachary J., et al. "Homogeneous oligomers of pro-apoptotic BAX reveal structural determinants of mitochondrial membrane permeabilization." *Molecular cell* 79.1 (2020): 68-83.

30. Westphal, D., R. M. Kluck, and G. Dewson. "Building blocks of the apoptotic pore: how Bax and Bak are activated and oligomerize during apoptosis." *Cell Death & Differentiation*21.2 (2014): 196-205.

31. Czabotar, Peter E., et al. "Bax crystal structures reveal how BH3 domains activate Bax and nucleate its oligomerization to induce apoptosis." *Cell* 152.3 (2013): 519-531.

32. Dengler, Michael A., et al. "BAX activation: mutations near its proposed non-canonical BH3 binding site reveal allosteric changes controlling mitochondrial association." *Cell Reports*27.2 (2019): 359-373.

33. Wang, Kun, et al. "Mutagenesis of the BH3 domain of BAX identifies residues critical for dimerization and killing." *Molecular and cellular biology* 18.10 (1998): 6083-6089.

34. Adachi, M., and K. Imai. "The proapoptotic BH3-only protein BAD transduces cell death signals independently of its interaction with Bcl-2." *Cell Death & Differentiation* 9.11 (2002): 1240-1247.